REVIEWS

Structural evolution and membrane interactions of Alzheimer's amyloid-beta peptide oligomers: New knowledge from single-molecule fluorescence studies

Robin D. Johnson,[1,2] Duncan G. Steel,[1,3,4] and Ari Gafni[1,5]*

[1]Department of Biophysics, The University of Michigan, Ann Arbor, Michigan 48109
[2]University of Michigan Medical School, The University of Michigan, Ann Arbor, Michigan 48105
[3]Department of Electrical Engineering and Computer Sciences, The University of Michigan, Ann Arbor, Michigan 48105
[4]Department of Physics, The University of Michigan, Ann Arbor, Michigan 48105
[5]Department of Biological Chemistry, The University of Michigan, Ann Arbor, Michigan 48105

Received 23 March 2014; Revised 15 April 2014; Accepted 17 April 2014
DOI: 10.1002/pro.2479
Published online 19 April 2014 proteinscience.org

Abstract: Amyloid-β peptide (Aβ) oligomers may represent the proximal neurotoxin in Alzheimer's disease. Single-molecule microscopy (SMM) techniques have recently emerged as a method for overcoming the innate difficulties of working with amyloid-β, including the peptide's low endogenous concentrations, the dynamic nature of its oligomeric states, and its heterogeneous and complex membrane interactions. SMM techniques have revealed that small oligomers of the peptide bind to model membranes and cells at low nanomolar-to-picomolar concentrations and diffuse at rates dependent on the membrane characteristics. These methods have also shown that oligomers grow or dissociate based on the presence of specific inhibitors or promoters and on the ratio of Aβ40 to Aβ42. Here, we discuss several types of single-molecule imaging that have been applied to the study of Aβ oligomers and their membrane interactions. We also summarize some of the recent insights SMM has provided into oligomer behavior in solution, on planar lipid membranes, and on living cell membranes. A brief

Abbreviations: AD, Alzheimer's Disease; ADDL, amyloid-derived diffusible ligand; Aβ, amyloid-β peptide; Aβ40, 40-residue version of Aβ; Aβ42, 42-residue version of Aβ; Aβ*56, dodecameric Aβ oligomer; APP, amyloid precursor protein; cTCCD, confocal two-color coincidence detection; D, diffusion coefficient; FAM, carboxyfluorescein; FRAP, fluorescence recovery after photobleaching; FRET, fluorescence resonance energy transfer; GUV, giant unilamellar vesicle; hAPP, human Amyloid Precursor Protein; HFIP, hexafluoroisopropanol; HL488, HiLyte Fluor 488; HL555, HiLyte Fluor 555; HL647, HiLyte Fluor 647; MSD, mean square displacement; SMM, single-molecule microscopy; TAMRA, carboxytetramethylrhodamine; TIRF, total internal reflection fluorescence.

Grant sponsor: National Institutes of Health (NIH); Grant numbers: R21-AG033749; R21-AG027370. Grant sponsor: University of Michigan Medical Scientist Training Program; Grant number: T32-GM07863.

*Correspondence to: Ari Gafni, 3204 Chemistry, Box 1055, 930 N. University Avenue, Ann Arbor, MI 48109. E-mail: arigafni@umich.edu

overview of the current limitations of the technique, including the lack of sensitive assays for Aβ-induced toxicity, is included in hopes of inspiring future development in this area of research.

Keywords: Alzheimer's disease; amyloid-beta peptide; oligomers; single-molecule microscopy; fluorescence; peptide-membrane interaction

Introduction

Amyloid-β (Aβ) is a peptide ranging from 39 to 43 residues in length produced by cleavage of an integral membrane protein, the amyloid precursor protein (APP).[1] The Aβ is present in both normal and Alzheimer's disease (AD) human brain tissue, albeit at low (from picomolar to nanomolar) concentrations.[2,3] Aβ40 is the more abundant, less amyloidogenic form of the peptide, normally constituting about 90% of the soluble Aβ pool. The remaining 10% of the peptide is mostly Aβ42, a more amyloidogenic form with two additional hydrophobic residues at the C-terminus. Monomeric Aβ is thought to be predominantly unstructured in solution; the middle segment of the peptide in particular likely samples a wide ensemble of conformations, depending on conditions.[4,5] At low concentrations present *in vivo*, the oligomeric state of the peptide is also likely to be in a constant state of flux, with small aggregates (from monomers to hexamers) interconverting in a dynamic equilibrium.[6–8] Aggregation is characterized by an initial lag phase during which aggregation is slow but where oligomeric "seeds" form. These then add peptide monomers in a rapid, nucleation-dependent fibrilization to form a mixture of fibrils and small oligomers in a stable equilibrium. The resulting cross-β sheet-rich fibrils represent the primary component of the plaques originally identified by Alois Alzheimer in the brains of patients afflicted with AD.[9]

The past 20 years have brought about a major paradigm shift in the AD field. Since Alzheimer's initial discovery of amyloid plaques, research had focused on Aβ fibrils as a likely causative factor for the clinical symptoms of AD, an idea referred to in the literature as "the amyloid hypothesis." More recently, however, emerging evidence has prompted a transition to an "amyloid oligomer hypothesis."[10–12] Plaque load and insoluble Aβ aggregates correlate poorly with AD symptoms when compared with soluble Aβ levels and synapse loss,[13–15] and oligomers have largely been found to induce greater toxicity to cultured cells than comparable quantities of fibrils.[16–18] These findings and others suggest that small soluble oligomers of Aβ may be the critical neurotoxic species of the peptide.

Experimental

A number of groups have begun to utilize a unique fluorescence microscopy-based biophysical toolset (single-molecule microscopy, or SMM) to further explore the structure and function of the Aβ oligomers. Studying these aggregates by single molecule fluorescence techniques offers advantages over ensemble methods because of the level of detail of the data obtained. If behavior of a small population in a sample is responsible for a large downstream effect, the dominating signal from the majority can obscure the connection.[19] Populations that make comparatively small contributions to the overall signal are ignored. With single molecule techniques, the behavior of individual particles is monitored and classified, greatly reducing the chances that such important relationships in the data will be overlooked.[20]

Beyond this general rationale, studying Aβ oligomerization and membrane binding at physiological peptide concentrations presents a number of challenges that SMM is uniquely suited to overcome. Soluble Aβ is only found at nanomolar to picomolar levels in the human brain.[2,3] Although this can be an obstacle for many traditional ensemble biochemical methods, such very low probe concentrations are required to reach the low fluorophore density needed to resolve single molecules. Efforts to pinpoint the neurotoxic aggregates have also been complicated by the finding that at physiological concentrations, Aβ exists as a mixture of metastable species.[6–8] Single-molecule microscopy (SMM) experiments can be conducted with milliseconds-to-minutes temporal resolution, offering a window into changes that occur on this time scale. The data are snapshots of the distribution of Aβ species that exists at a certain moment in time, and when aggregates exhibit structural transitions, these changes can be visualized. Finally, since Aβ-membrane interactions are complex and variable, binding sites may include a number of membrane integral receptors and specific lipid moieties. Binding affinity and membrane permeabilization may be strongly affected by factors such as membrane curvature and charge.[21] The membranes of neuronal cell somas, neurites, dendritic spines, and postsynaptic densities are distinctive, chemically and morphologically.[22–24] It follows that Aβ may have widely varying binding behavior and membrane effects in different cellular membrane compartments. SMM allows precise visualization of individual oligomers and their on-cell locations. Additionally, with the wide variety of fluorescent probes available, SMM can easily be used to

determine whether particular membrane molecules may be acting as Aβ binding sites.

In the past five years, SMM explorations of Aβ oligomer size, composition, and membrane interactions have been conducted through several different approaches, some of which are illustrated in Figure 1. Single-molecule photobleaching, through total internal reflection fluorescence [TIRF, see Fig. 1(A)] or confocal geometry, has been used by our group and others to elucidate the size distribution of Aβ oligomers at physiological (picomolar–low nanomolar) concentrations in solution,[8,25] confirming that very small oligomers predominate at these concentrations. In this approach, a single fluorophore is covalently linked to each peptide monomer. When an oligomer of such labeled monomers is illuminated at the appropriate intensity, the fluorophores bleach one at a time, creating a stepwise intensity-versus-time trajectory in which each step corresponds to the bleaching of a single monomer, as shown in Figure 1(C). The method is somewhat limited in that for oligomers larger than hexamers, or so, photobleaching trajectories begin to resemble an exponential decay. This tendency increases with the size of the oligomer, so that distinguishing individual photobleaching steps (and therefore, accurately measuring size) becomes difficult for very large oligomers.

More recently, we have studied how oligomer growth on a membrane occurs at near-physiological concentrations for Aβ40, Aβ42, and mixtures of the two by using single particle confocal-mode peak fluorescence intensity and fluorescence integrated intensity measurement [methods illustrated in Fig. 1(D)].[26–28] In the peak fluorescence intensity method, the peak fluorescence intensity of a detected particle is divided by the fluorescence intensity of a monomer to yield an estimated oligomer size.[26] Similarly, in the integrated intensity measurement method, the average fluorescence intensity of a monomer in solution is obtained by measuring the fluorescence intensity of standards containing a known number of fluorophores per volume unit.[27] The total fluorescence intensity of a detected particle within a volume unit is then divided by this average monomer fluorescence intensity to obtain an oligomer size. These two methods enabled us to measure the sizes of oligomers containing more than six subunits. We have also combined these methods with single molecule fluorescence resonance energy transfer (FRET) measurements to show that Aβ40 and Aβ42 directly interact to form mixed oligomers.[28]

The confocal two-color coincidence detection (cTCCD) method for oligomer detection has also proved to be a powerful technique for exploring the oligomer–monomer equilibrium under different conditions.[29] In this method, illustrated in Figure 1(B), peptide monomers are labeled with one of two different fluorophores, with blue and red fluorescence, respectively, and mixed before being allowed to diffuse through the overlapped confocal volumes of two separate lasers. Fluorescence emission pulses occurring in only one fluorophore's emission band are counted as monomers, whereas simultaneous fluorescence emission pulses occurring in both fluorophores' emission bands are counted as oligomers. This preliminary "oligomer count" can then be corrected to account for chance simultaneous detection of multiple monomers labeled with different fluorophores. A correction is also made in this measurement for oligomers containing subunits labeled with only one fluorophore, which are not detected by the method.

To determine apparent oligomer size by cTCCD, the fluorescence intensity of each detected oligomer in the blue channel is measured, divided by the average intensity of a monomer, and doubled. For a large population in which the identity of the label does not affect binding affinities, this analysis should produce a representative size distribution. In calculating apparent size distributions, Narayan *et al*. correct for chance coincidence detection of monomers with different labels (mentioned earlier) as well as for estimated changes in fluorophore emission due to intraoligomeric FRET.[30] Despite such corrections, when size distributions obtained by cTCCD are compared with those obtained by single molecule TIRF fluorescence intensity measurement, the cTCCD method does result in detection of slightly fewer dimers-to-tetramers in comparison to the TIRF method (normalized fraction 62–63% vs. 80% with TIRF). This method of oligomer size measurement may therefore be better suited for the study of samples predominantly consisting of larger oligomers (greater than 7–10 subunits in size). The TIRF- or confocal-based photobleaching and confocal integrated intensity measurement methods discussed earlier likely produce more accurate measurements of the size of the smallest oligomers (up to pentamers or hexamers).

The Dobson group and others have also begun to explore oligomer mobility on membranes using single-particle tracking techniques [Fig. 1(E)] in which the two-dimensional trajectories of single particles over time are used to extract diffusion coefficients and other parameters.[31,32] These can then be used to classify the particles' motion and make inferences regarding their sizes, interactions with other proteins, and membrane interactions.

This review will focus on the insights obtained into Aβ oligomer formation, structure, and interactions with other biomolecules through recent SMM work. We will also discuss how these results contribute to the mechanistic understanding of Aβ's membrane binding behavior. Finally, the current

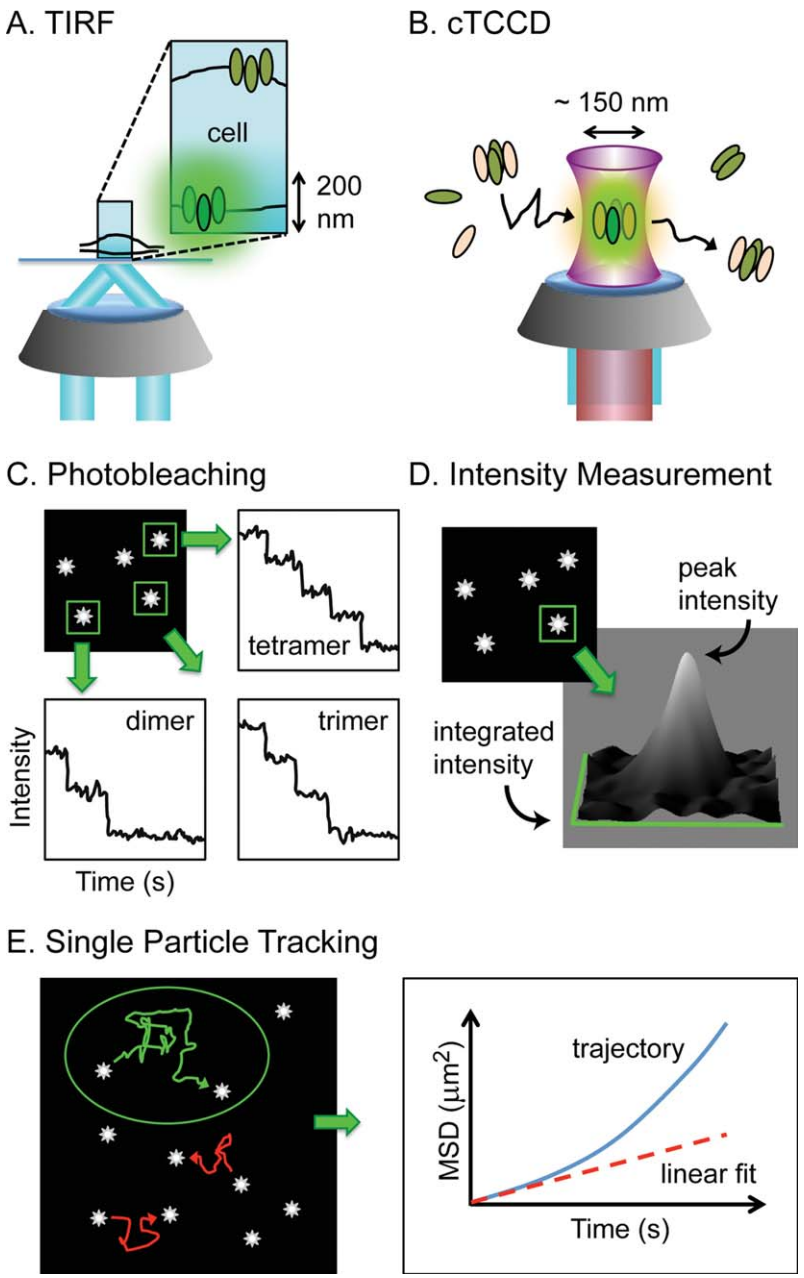

Figure 1. Summary of SMM methods discussed in this review. A: In total internal reflection fluorescence (TIRF) microscopy, a high numerical-aperture lens is used to reflect laser light off a glass slide, creating an evanescent excitation wave within the first 100–200 nm above the slide in z-direction. This technique enables selective excitation of fluorescently labeled Aβ peptides (green ellipses) adherent to the basal cell membrane or within the basal cell cytoplasm. B: In confocal two-color coincidence detection microscopy (cTCCD), solution samples of Aβ peptides are imaged in confocal mode. Each peptide is singly labeled with one of two different fluorophores (orange and green ellipses in the image), and the sample is illuminated at each fluorophore's respective excitation wavelength simultaneously. Oligomers moving through the confocal volume are identified by coincident fluorescent emission from both fluorophores. Monomers diffusing through the volume will emit only in one emission band. C: Schematic of fluorescently labeled oligomers in the microscopy field and how the photobleaching trajectories of some specific oligomers might appear, including background fluorescence level and noise. Counting the steps in a single oligomer photobleaching trajectory reveals the number of fluorophores—and therefore monomeric subunits—in each oligomer. A dimer's trajectory has two photobleaching steps to bleach completely down to the background level, a trimer has three, a tetramer has four, and so on. These studies can be conducted in TIRF or confocal laser scanning geometries. D: Diagram showing a region of interest around a single oligomer (shown zoomed in at right as a smoothed three dimensional surface plot of an actual cell-bound oligomer from Ref. 62). Confocal mode peak fluorescence intensity or integrated fluorescence intensity of the oligomer's intensity profile can be used to measure oligomer size. E: In the single particle tracking method, paths of particles in motion are tracked over time. These trajectories are used to measure mean square displacement at each time point. The graph at right illustrates how a trajectory for a particle exhibiting "directed" type motion might appear (see Ref. 31 for further details). The diffusion coefficient of the particle can be obtained by calculating the slope of linear fit of the first 2–5 points on this curve.

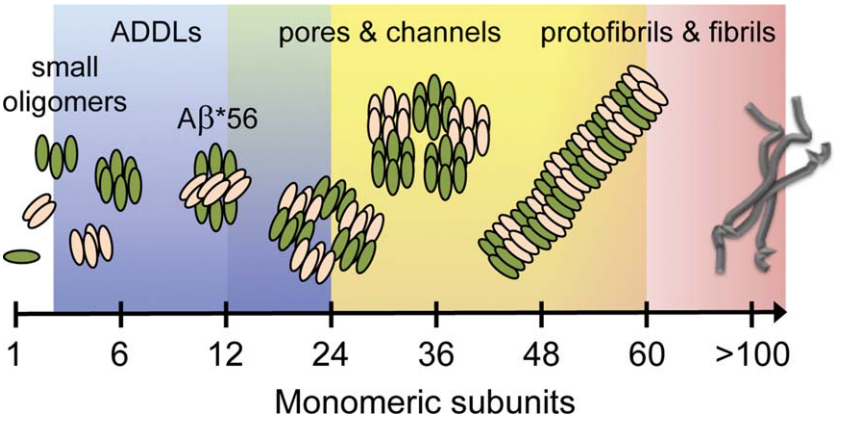

Figure 2. Several types of amyloid-β oligomers have been identified in the literature. These include small oligomers (dimers to hexamers), amyloid-derived diffusible ligands (ADDL's), the Aβ dodecamer Aβ*56, various ion-conducting pores and channels identified through electrophysiology and atomic force microscopy, and annular and linear protofibrils. Estimated size ranges for ADDL's, pores/channels, and protofibrils to fibrils are shown in blue, yellow, and red respectively.

limitations of SMM will be covered with the goal of outlining areas in which further innovation could substantially advance AD research.

Amyloid-Beta Oligomer Structural Evolution

Current evidence implicates a number of different types of oligomers in the neuronal dysfunction that features in AD, some of which are depicted in Figure 2. Aβ dimers and trimers purified postmortem from human AD brain tissue and from the medium of cells expressing human APP have recently been shown to induce deficits in long-term potentiation and increases in long-term depression.[33,34] The ratio of Aβ40 to Aβ42 in these oligomers was not characterized. Another recent study indicated that Aβ40 dimers, trimers, and tetramers exhibited nonlinear increases in cellular toxicity with molecular weight.[16]

Amyloid-derived diffusible ligands, or ADDL's, generally prepared from synthetic Aβ42, contain oligomers from 10 kDa to 100 kDa in molecular weight, or roughly trimers to 24-mers.[35] These small globular aggregates have been shown to bind specifically to synapses, reduce dendritic spine density, and alter normal tau sorting and localization.[36–38] Similarly sized spherical oligomers, also prepared *in vitro* and containing an estimated 10–24 subunits each, have been shown to cause immediate, catastrophic calcium leakage in SH-SY5Y neuroblastoma cells.[17] Of note, both preparation protocols require exposure of the peptide to hexafluoroisopropanol, a potentially membrane-toxic solvent, effects of which will be discussed in more detail in the following.[39]

In 2006, Lesne *et al*. detected an Aβ42 dodecamer in the brains of hAPP-expressing transgenic mice that appeared to correlate well with memory deficits.[40] Once purified and injected into the brains of young mice, this aggregate (termed Aβ*56) caused long-term memory deficits, as measured by the Morris water maze. However, this species was not detected in Aβ purified from human AD brain.[34,41]

Several reports in the 1990's indicated that freshly solubilized Aβ was capable of forming cation-selective ion channels with stepwise conductances in biological membranes.[42,43] Pore-like protofibrillar structures formed from Aβ and other amyloid-forming peptides were later detected by electron microscopy and atomic force microscopy.[44–46] The imaged "annular protofibrils" were generally in the range of 10–20 nm in diameter, with 1–2 nanometer central pores, and appeared to contain between four and six distinct subunits, each likely containing multiple peptide monomers. These data were interpreted as evidence that Aβ and other amyloid-forming peptides may disrupt membranes in the same fashion as bacterial pore-forming peptides.[45] Most discussions of these annular structures place their probable size between 12 and 60 monomeric peptides.

Importantly, the vast majority of these aggregates have been either purified from mammalian tissue or chemically prepared *in vitro* at high concentrations, providing little insight into how such structures form and evolve at physiological concentrations of Aβ.

SMM was first applied to this problem by Dukes *et al*.[25] Biotinylated FAM-labeled Aβ40 was first solubilized to 0.2–1 μ*M*, then diluted to 30 p*M* and allowed to tether to streptavidin-functionalized coverslips. Imaging was performed in solution by confocal scanning microscopy. Oligomer size distributions for these samples, generated by the single-molecule photobleaching method, consisted of mostly monomers and dimers (each representing roughly 45% of detected particles) with fewer trimers (7%) and a smaller proportion (around 2%) of "unmeasurable" oligomers greater than pentamers. To further test the method, size distributions were obtained for

samples treated with aggregation-promoting conditions (aging of samples, acidic pH, 4:1 $ZnCl_2$:Aβ40 concentrations) or with aggregation inhibiting conditions (in the presence of a β-sheet disrupting peptide or the zinc chelator clioquinol). Importantly, oligomer size distributions under these conditions generally exhibited shifts in the expected directions, with greater numbers of trimers to pentamers as well as oligomers greater than pentamers being observed under pro-aggregation conditions. The addition of the β-sheet disrupting peptide or clioquinol to Aβ exposed to zinc or low pH significantly shifted the distributions back toward monomer–dimer predominance. As the biotinylated FAM-labeled Aβ40 was not compared with native peptide, these results were of somewhat limited scope, but the study thoroughly demonstrated the potential of SMM for future study of modifiers of peptide aggregation.

We pursued an alternate method of peptide immobilization for SMM studies of fluorescently labeled Aβ40.[8] HiLyte Fluor 488 (HL488)-labeled Aβ40 in solution at around 100 n$\underline{M}$ was further diluted to concentrations of 0.1–1 nM, spin-coated onto kilned coverslips, and the dry samples were imaged by confocal scanning microscopy. In this work and another study, we have demonstrated that the fluorophore did not alter the ability of Aβ40 to form fibrils and permeabilize membranes relative to unlabeled Aβ40.[26]

Initial experiments showed that the spin-coating SMM method could easily differentiate between a gel-chromatography filtered sample containing predominantly monomers and dimers and an unfiltered sample containing a wider distribution of oligomers. Subsequently a number of methods were used to further refine and test the accuracy of the distributions. First, as spot-detection required setting an arbitrary detection threshold, simulated trajectories were analyzed to determine the number of small oligomers that were escaping detection at the utilized threshold values, and a correction was applied to the distributions to account for this. Corrected size distributions obtained by our SMM protocol for fluorescently labeled parvalbumin were compared to distributions obtained by mass spectroscopy and found to agree closely.[8] Corrected SMM distributions for HL488 Aβ40 also agreed with distributions obtained by fitting multiple Gaussians to gel filtration elution profiles for Aβ40. This approach thus provides a verified, accurate snapshot of small oligomer size distributions at the time of spin-coating. Baseline size distributions obtained for Aβ40 under these conditions were shifted slightly towards dimers, trimers, and tetramers when compared with the distributions observed by Dukes *et al*.[8,25] Given the similarities in behavior between HL488 Aβ40 and unlabeled Aβ40, these results likely do apply to endogenous peptide. Like Dukes *et al*., we did observe a small population of oligomers that were much larger than hexamers in size.[8,25] Although easily detected, the sizes of these oligomers cannot be accurately measured by single-molecule photobleaching. Overall, the results of our studies and those of Dukes *et al*. were quite similar, with the samples predominantly consisting of monomers (30–50% of particles), dimers (40–50% of particles), and some trimers and tetramers.[8,25]

A SMM approach that better estimates the proportion and sizes of much larger oligomers has been developed by the Dobson laboratory. Narayan *et al*. used confocal two-color coincidence detection (cTCCD), described in the Introduction, to characterize the proportion of oligomers present in samples of HL488 Aβ40 and HiLyte Fluor 647 (HL647)-labeled Aβ40 aggregated for up to 20 hours at pH 7.4, 37°C, at either 10–30 nM or 600 n$M-2$ μM.[30] Samples were then diluted to 25–50 pM for cTCCD experiments. Interestingly, in contrast to the results discussed earlier, only about 1% of the particles detected were found to be oligomeric by cTCCD. Of the oligomeric particles detected, Narayan *et al*. found only 50% to be dimers to tetramers in size, with the remaining oligomers being pentamers or larger.[30] Aggregation concentration (10–30 nM vs. 600 n$M-2$ μM) did not significantly affect the distribution.

Given the difficulties inherent in working with Aβ and the differences in methods among groups, quantitative disparities between different laboratories are almost certainly less important than qualitative similarities of the data across groups. Even qualitatively, however, the results obtained by our lab and the Lammi group differ from those of Narayan *et al*.[8,25,30] Oligomers detected by Ding *et al*. and Dukes *et al*. included fairly equal mixtures of monomers and dimers with smaller but significant populations of trimers-tetramers, and much smaller populations (<10% of particles) of very large oligomers.[8,25] In Narayan *et al*.'s study, less than 1% of solution particles represented oligomers, and of those oligomers, roughly 50% were greater than tetramers in size.[30]

A number of factors may contribute to this difference. The greater numbers of dimers, trimers, and tetramers detected by Dukes *et al*. and Ding *et al*. may be due to "seeding" of small oligomers by surface interactions in the previously discussed experiments.[8,25] Monomers may be more likely to interact with monomers which are already surface-bound, an effect which would not be observed in cTCCD, an assay based on monitoring diffusion of free particles through solution volumes. This is especially important to consider given that membrane binding has frequently been shown to promote or "seed" Aβ oligomer growth. An additional rationale

for the difference between the cTCCD method results and the single molecule photobleaching results is that the peptide preparation method differs vastly between the two labs. The studies by both Ding *et al*. and Dukes *et al*. used lyophilized peptide freshly dissolved to 0.1–1 μM in sodium phosphate buffers at room temperature or 4°C and then diluted to picomolar or nanomolar concentrations before sample preparation.[8,25] Conversely, Narayan *et al*., before imaging used an aggregation protocol in which samples at 10–30 n*M*, 600 n*M*, or 2 μ*M* were heated to 37°C and incubated in solution until fibrils were detected.[30] The population of smaller oligomers (dimers to hexamers) in these samples may be rapidly depleted by their addition to larger oligomers or fibrils. Despite differences in peptide treatment and results, all three studies do provide direct visual evidence that oligomers form and exist in a stable equilibrium at nanomolar-to-picomolar Aβ concentrations.

The utility of SMM methods for study of Aβ in solution at very low concentrations extends well beyond the determination of which oligomers are present in such conditions. As predicted by Dukes *et al*., SMM methods have now been used to study the effects of aggregation inhibitors on oligomers at physiological or near-physiological concentrations.[25,30,47] Peptide-based inhibitors with central sequences similar to Aβ's hydrophobic amino acids 16–21 have been shown to slow fibrillogenesis and reduce neurotoxicity in ensemble experiments.[48–51] To examine their effects on small oligomer evolution, FAM-labeled, biotinylated Aβ40 oligomer distributions were first characterized under proaggregation conditions (pH 5.8 or 4:1 zinc:Aβ ratio).[47] Distributions were then measured again in the presence of four such peptide-based inhibitors. Incubation with 10:1 inhibitor: Aβ40 concentrations of any of these four peptides significantly shifted the distributions of small oligomers toward monomers under acidic or zinc-rich conditions. At reduced concentrations, two of the peptides were more effective inhibitors in acidic conditions, whereas the remaining two were more effective in the presence of zinc. Since proposed inhibition mechanisms differ for each inhibitor, these results can be used to make inferences about the chemical nature of small oligomer formation and dissociation under each condition.

Single-molecule exploration of the effects of chaperone protein inhibitors on Aβ oligomer formation has also been conducted. The extracellular chaperone protein clusterin was shown to greatly inhibit oligomer formation in cTCCD experiments performed by Narayan *et al*.[30] Complexes containing both clusterin labeled with AlexaFluor 647 and HL488 Aβ were detected in similar quantities to Aβ oligomers at coincident time points, indicating that clusterin was likely directly binding to oligomers. Furthermore, in fibril disaggregation reactions, clusterin was found to increase the overall final concentration of oligomers and decrease the overall monomer concentrations, in effect stabilizing the oligomers shed by fibril dissociation. Subsequently, similar methods were used to show that an intracellular chaperone, αB-crystallin, bound to and stabilized oligomers in similar fashion, though with a shorter half-life (17 hours versus 50 hours for the extracellular clusterin).[52] These experiments were performed at 1:1 molar chaperone: Aβ monomer ratio, which is likely equal to or less than the physiological chaperone: Aβ ratio. The results provide an elegant insight into one potential mechanism by which the body normally clears toxic Aβ oligomers.

Membrane Binding Affects Oligomer Formation: Model Membranes

The role of membrane interactions in the formation of toxic Aβ oligomers is a subject of debate. We note that for *in vitro* experiments like those discussed here, toxicity itself is difficult to define, as the precise mechanism by which Aβ damages cells is as yet unknown. Cell viability assays represent by far the most popular method for toxicity assessment.[16,18,53–55] However, this method has the disadvantage of being the last possible indication of the peptide's toxic effects. Electrophysiological methods for assessing neuronal dysfunction and membrane conductivity are also commonly utilized to detect more subtle, earlier detrimental effects of Aβ exposure. Observed electrophysiological signs of Aβ-induced toxicity have included decreased firing frequency on multielectrode arrays, decreased long-term potentiation, and simply ion leakage across membranes.[26,34,56–58] Increased intracellular calcium concentration and abnormal synaptic spine density and morphology have also gained acceptance as signs of Aβ-induced toxicity.[17,27,37,59,60] Therefore, for the purposes of the current discussion, Aβ-induced toxicity refers to results obtained by any of these methods of assessing cellular death or dysfunction.

A number of groups have found that Aβ preaggregated at high concentrations induces greater toxicity than monomeric or fibrillar Aβ, implying that oligomers formed at high concentration in solution (without contact with biological membranes) are capable of interacting with cell membrane moieties.[17,53] Although Aβ may be present locally at μM concentrations, the global presence of only nanomolar concentrations provokes the question of whether oligomers formed at very high concentrations are physiologically relevant. Additionally, these reports to some degree contradict older evidence that treatment of biological membranes with unaggregated Aβ leads to formation of cation-selective, stepwise conductance changes.[42,43] The recent usage of membrane-damaging solvents in Aβ peptide

preparation has further complicated these questions. Demuro *et al*. in 2005 reported that oligomers prepared *in vitro* produced immediate, catastrophic calcium leakage in SH-SY5Y cells.[17] The peptide used in these experiments, however, had been treated with hexafluoroisopropanol (HFIP) before the oligomerization protocol.[17] A later study showed that traces of the HFIP may have remained in the oligomerized samples following evaporation, destabilizing membranes, and effectively inducing calcium leakage.[39]

Understanding the relative importance of specific Aβ oligomers in the mechanism of toxicity requires a better knowledge of which oligomer types form and interact with membranes at low concentrations (in the absence of membrane-disrupting solvents). We must also improve our understanding of how oligomers formed in solution are related to those formed in contact with membranes under different conditions. The use of single molecule fluorescence imaging enables direct visualization of membrane-bound monomers and oligomers in multiple environments and has already helped shed light on these questions.

In our studies of monomeric Aβ40's interactions with anionic lipid bilayers, we showed that binding and oligomerization occur in two separate phases.[61] Briefly, planar membranes composed of a 1:1 ratio of 1-palmitoyl-2-oleoyl-sn-glycero-3-phosphocholine (POPC) to 1-palmitoyl-2-oleoyl-sn-glycero-3-[phospho-rac-(1-glycerol)] (POPG) were incubated with concentrations of 2–100 n*M* HL488 Aβ40 for up to 6 days.[61] The use of anionic membranes was motivated by results of ensemble experiments performed in our laboratory and by others indicating that negatively charged membranes bind Aβ more tightly and become especially susceptible to permeabilization by the peptide.[21] Across this concentration range, initial monomer binding occurred uniformly at an estimated density of $\sim 9 \times 10^8$ monomers per cm^2. Binding exhibited first-order kinetics and was essentially irreversible, with a k_{off} rate less than 2×10^{-6} s^{-1}. The dissociation constant for this concentration regime was calculated to be <470 pm. The bound monomers were highly mobile, with fluorescence recovery after photobleaching (FRAP) experiments revealing that both the lipid molecules and the uniformly bound, diffusing monomeric Aβ40 had diffusion coefficients around 2 $\mu m^2/s$. The appearance of immobilized oligomers occurred within as little as 2.5 hours on membranes exposed to 100 n*M* solution of Aβ40. However, immobilized oligomers were not observed for several days on membranes exposed to 2 n*M* peptide or preincubated for 1 day with 2 n*M* peptide and then maintained in solution without Aβ. A much greater population of very large oligomers (estimated size 30–160 monomeric subunits) was observed in the 100 n*M* population, with the 2 n*M* population containing primarily dimers to dodecamers. Membranes pretreated with 2 n*M* peptide and then imaged after an additional 4.5 days' incubation at 0 n*M* or 2 n*M* peptide had nearly equivalent immobile oligomer densities. However, immobile oligomer density was roughly three times higher at the 100 n*M* concentration. We concluded that at very low solution peptide concentrations, membrane-bound oligomers formed primarily by association of the diffusing membrane-bound monomer population rather than by direct insertion from solution.[61] At higher concentrations, however, a large portion of the membrane-bound oligomers had to form either by direct insertion of preformed oligomers from solution or by rapid replenishment of the membrane-bound monomers used in oligomer formation by solution monomers.

Combining SMM with other electrophysiological or optical techniques allows one to correlate the presence of specific bound oligomers with ion movement across membranes. Our group performed such studies using "black lipid" membranes (prepared from a 7:3 ratio of diphytanoylphosphatidylcholine to diphytanoylphosphatidylserine) incubated with 10 n*M* to several hundred nanomolar solutions of HL488 Aβ40.[26] Similar initial binding of a uniform, diffusing monomer population was observed, with binding density estimated at 5×10^8 monomers per cm^2. This population was not found to induce ion conductance in the membrane. In fact, conductivity was only observed when immobile oligomers of size greater than pentamers to octamers were present, and it was found to increase in the presence of larger oligomers. The intermediate-sized oligomers were found to be stable, remaining immobile for several hours in the black lipid membrane. At very high (>200 n*M*) peptide concentrations, a third type of membrane-bound peptide aggregates was observed. These aggregates were much larger than the optical diffraction limit, changed significantly in size and structure over the course of several hours, and massively disrupted the membranes. Thioflavin T binding experiments performed using unlabeled peptide under conditions consistent with formation of both intermediate-sized oligomers and the much larger aggregates indicated that both classes of peptide aggregates possess significant β-sheet structure.[26]

Insight from model membrane experiments thus indicates that at very low concentrations (on the order of 1 n*M*), Aβ oligomer formation occurs primarily by association of membrane-bound, rapidly diffusing monomers.[61] However, at higher concentrations, direct insertion of solution-formed oligomers may occur. Intermediate sized-oligomers appear to be generally immobile within planar model membranes, possibly due to full insertion through the bilayers and interactions with the underlying slides.

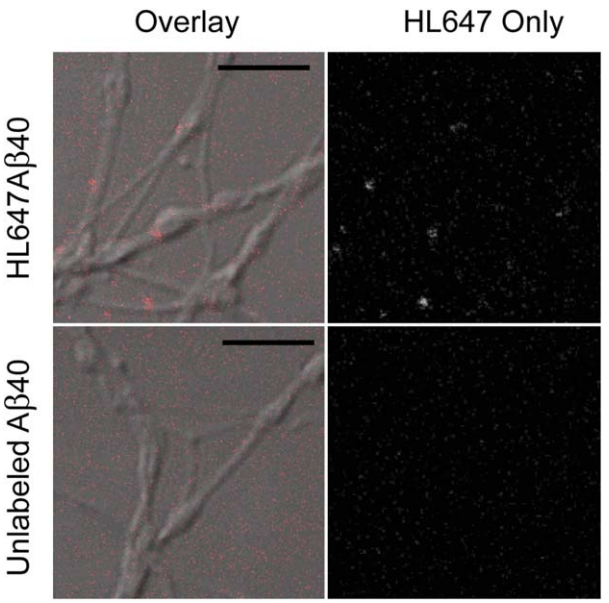

Figure 3. Neurites of primary rat hippocampal cells treated for 10 minutes with 1 n*M* HL647 Aβ40 (top row) show puncta of high fluorescence intensity corresponding to labeled monomers and oligomers. Cells treated with unlabeled Aβ40 (bottom row) were used as controls. Scale bars, 5 μm.

Furthermore, oligomers containing more than five to six monomeric subunits may be capable of allowing ion conductance across membranes, and these intermediate-to-larger sized oligomers have some β-sheet structure.[26]

Binding and Oligomer Formation: Live Cell Membranes

Characterizing Aβ's interactions with model membranes has yielded significant quantitative data on peptide binding and oligomer formation over hours-to-days. However, model membranes are significantly less complex in composition and dynamics than live cell membranes. To gain insight into how these factors affect Aβ-membrane binding and oligomer formation, we applied 50 n*M* HL647 Aβ40 peptide to SH-SY5Y neuroblastoma cells and imaged the cells after a 10-minute incubation.[27] Immobile oligomer size was determined by integrated fluorescence intensity measurement. Interestingly, under these conditions, we did not find evidence of a uniformly bound, diffusing population of monomers. However, immobile, cell surface-localized oligomers ranging in size from dimers to hexamers and larger were detected. These results led us to conclude that properties of the cell membrane must facilitate rapid in-membrane oligomer growth or preferential binding of oligomers over monomers.

Consistent with this hypothesis, the observed structures were found to be slightly larger in size than the oligomers nonspecifically bound to glass slides under the same conditions.[27] Although brief incubation in cell growth medium on glass slides did appear to induce increased Aβ40 oligomerization when compared with Aβ40 spin-coated from buffer, cell-bound oligomers were even greater in size. The majority of cell-bound oligomers colocalized with a membrane-specific dye. About 10% of cells loaded with a fluorescent calcium indicator did exhibit minor fluorescence increases within the first 10 minutes of exposure to 50 n*M* labeled or unlabeled Aβ40. We concluded that on cells, as on black lipid membranes, the observed small oligomers may induce very low-level calcium conductivity. Occasionally, very high intensity fluorescent structures, composing less than 10% of the total fluorescent particles, were also observed on cells in these experiments and likely represented aggregates containing greater than 20 peptide monomers.[27]

Further experiments using neurites of primary rat hippocampal cells gave initially similar results at even lower Aβ concentrations.[62] Plated cells were incubated with 1 n*M* HL647 Aβ40 or Aβ42 for 10 minutes, gently washed three times so as to preserve the cells' adherence to the slides, and imaged in confocal mode. Generally immobile small oligomers of HL647 Aβ40 were detected on cell neurites within 10 minutes incubation at 1 n*M*, as depicted in Figure 3. The size distribution for HL647 Aβ42 oligomers was similar. Interestingly, further incubation of the cells without solution peptide for up to 48 hours resulted in a small but significant decrease in on-membrane oligomer size and a decrease in the total amount of peptide bound. Prolonged incubation of the cells with peptide in solution resulted in no significant change to the size distribution for Aβ40, but a significant (if small) shift toward larger oligomers for Aβ42. In addition, we recently obtained very similar results using 2 n*M* HL555 Aβ40 and 2 n*M* HL647 Aβ42, the only difference being a slight trend toward larger oligomers in the 2 n*M* Aβ42 samples (likely a result of the doubled incubation concentration).[28] No toxicity was observed by assessment of calcium transient frequency, fluorescent calcium indicator activation, or spine density at 1 nM peptide exposure over these time scales.

An alternate approach to the study of Aβ interactions with live cell membranes has been taken by Narayan *et al*. using dual-excitation TIRF microscopy.[31] Similarly to cTCCD, in this method, samples of a 1:1 mixture of HL488 and HL647-labeled Aβ were coexcited with two lasers. Whereas in the cTCCD method, diffusion of both fluorophores at the same time through a confocal volume is counted as an oligomer, in this study, detection of both fluorophores at the same location in the TIRF *x-y* plane is counted as an oligomer. For the TIRF experiments, 1:1 mixtures of HL488 and HL647-labeled Aβ40 or Aβ42 were incubated at low micromolar

concentrations to promote in-solution formation of oligomers. This preaggregated peptide was applied to suspended mouse hippocampal cells at 500 n*M*. Following a 15-minute exposure, the cells were washed, centrifuged, resuspended, and allowed to reattach to polyethylene glycol-coated slides for 10 minutes. The proportion of cell-bound particles counted as oligomers was between 40 and 70% for Aβ42 and 10 and 40% for Aβ40. These were significantly higher proportions than for peptide in solution. Additionally, when oligomer sizes were estimated, the cell-bound oligomers for both peptides were found to be larger than oligomers in growth medium. For both peptides, ~40% of the cell-bound oligomers were greater than five subunits in size.

This represents a significant increase over the roughly 10% of peptide-bound particles we observed in this size range; the disparity is most likely due to the preaggregation of the peptide and the significantly higher peptide concentrations (500-fold) employed in these experiments.[27,31,62] Differences in binding affinity between small and large oligomers may also contribute, as the multiple washings described earlier might detach smaller oligomers. It is also possible (if somewhat unlikely) that resuspending the cells after Aβ exposure and allowing them to reattach selects for a subpopulation of cells that has larger Aβ aggregates bound. Additionally, the size distributions of oligomers may be affected by the part of the cell being imaged—our study focused on the neurites, whereas Narayan *et al*. examined cell soma.[31,62] Differences in membrane curvature and charge between these structures could significantly affect peptide binding and oligomerization.

Despite these differences, a key point is that both studies detected significantly larger oligomers on the membrane than in solution. As Narayan *et al*. suggest, this result may be due to preferential binding of oligomers in comparison to monomers.[31] Another explanation suggested by multiple previous studies is that membrane binding catalyzes oligomer formation from bound, diffusing monomers and very small oligomers. Interestingly, Narayan *et al*. do detect a small population of fast-diffusing, most likely monomeric species using single particle tracking methods.[31] We note that sparsely bound, rapidly diffusing monomer would not necessarily be detected above background in our confocal method, given the difficulty of detecting this lower signal in the context of cellular autofluorescence.[27]

As discussed earlier in the summary of the model membrane work, both mechanisms could certainly be at play, with direct binding from solution generally predominating at higher concentrations and in-membrane oligomer formation dominating at lower ones. As recently hypothesized by Zhang *et al*., Aβ oligomers formed from monomer within the membrane and those formed in solution (before membrane-binding) may even induce toxicity by two entirely separate mechanisms.[63]

Synergy of AB40 and AB42

A number of recent studies have raised interest in the role of Aβ42:Aβ40 ratio in peptide aggregation and interaction with cells.[55,56] We explored this issue by comparing on-membrane oligomer growth of a 1:1 mixture of the two peptides to that observed for each peptide alone.[62] Relative to homogeneous Aβ40 or Aβ42, the size distribution for cell-bound mixed 1 n*M* peptide after 10 minutes was significantly shifted toward monomers and dimers. Perhaps more intriguingly, a very significant oligomer size increase was observed for the mixed peptide after 24–48 hours at 1 n*M*. This increase was much larger than that observed for either peptide alone, with over 70% of the total peptide residing in oligomers greater than trimers after 1–2 days. Additionally, the total amount of peptide bound doubled for the mixed peptide over this time, indicating that much of this growth was due to new binding of peptide from solution. These results indicate that cells either (A) have a higher binding capacity for oligomers of the mixed peptide or (B) have a reduced ability to clear oligomers of the mixed peptide when compared with either Aβ40 or Aβ42 alone.

FRET experiments with HL555 Aβ40 and HL647 Aβ42 confirmed that mixed oligomers do in fact form.[28,62] Following this observation, we continued to utilize these two peptides to further examine the mechanism of oligomer growth on neurites exposed to mixed Aβ40 and Aβ42. We found that when cells were incubated with mixed peptide for a full 48 hours, the additional oligomer growth beyond that observed at 10 minutes could be accounted for primarily by increases in Aβ42 fluorescence. This suggests a mechanism by which mixed Aβ42:Aβ40 oligomers act as "seeds" for binding of additional Aβ42 subunits. Alternately, cells may have a reduced ability to clear mixed oligomers when compared with pure Aβ42 or Aβ40, allowing mixed aggregates to dwell at the membrane longer and in turn maximizing their ability to allow Aβ42 to bind. In either case, this is an intriguing result, as high Aβ42:Aβ40 ratio appears to result in earlier age of Alzheimer's disease onset in human brain,[64,65] and mutations in presenilins 1 and 2 that cause familial AD increase this ratio in transfected cells and transgenic mice.[66–68] It is difficult to draw conclusions at this point as to the structural explanation for this phenomenon. However, the observation does make clear that the presence of Aβ40 is necessary for the increased binding of Aβ42 over time. Further studies will be necessary to understand the molecular interactions involved.

Mobility on membranes

Surface mobility of membrane-bound oligomers is a question of significant interest. In our studies of neurite-bound Aβ40 and Aβ42, a large number (roughly 70%) of small oligomers were found to be immobile enough for fluorescence intensity measurement, which likely reflects a "confined" type of motion on the membrane. Several groups have looked into this question in more detail using single-particle tracking methods that allow diffusion coefficients to be extracted by fitting the initial 2–5 points of a mean square displacement (MSD) versus time plot.[31,32,69,70]

In one set of single-particle tracking experiments, Calamai *et al*. applied preaggregated Aβ42 to SH-SY5Y cells at 10 μ*M*. They then incubated the cells with antibodies specific for prefibrillar conformation (I11) and fibrillar conformation (OC) to label the bound oligomers with quantum dots for particle tracking.[32] While no measurement of oligomer size was obtained, I11 antibodies reportedly bind to oligomers from 8 kDa (dimers) to 100 kDa (25-mers), and OC antibodies bind to oligomers from 8 kDa (dimers) to 250 kDa (75-mers) in size. Fibrillar conformation (OC-labeled) oligomers tended to exhibit the least motion, with 75% of particles exhibiting a "confined" type motion as categorized by the curvature of their MSD versus time plot. Among the prefibrillar (I11-labeled) aggregates, 50% of particles had plots typical of "confined" motion, over 25% had plots typical of Brownian motion, and roughly 10% had plots typical of more rapid "directed"-type motion. Thus, the majority of oligomers overall exhibited highly restricted motion; median diffusion coefficients for prefibrillar (I11) and fibrillar (OC) aggregates, respectively, were 4×10^{-3} μm^2/s and 9×10^{-4} μm^2/s. Of note, diffusion coefficients obtained with TAMRA-labeled Aβ42 did not differ significantly from those obtained with quantum dot-labeled Aβ42, implying that the mobility is not affected by the size of the label. Calamai *et al*. suggest that the oligomers exhibiting "directed" motion may be contained in intracellular vesicles, a likely possibility given recent reports that extracellular Aβ can be taken up by cells.[18,71]

The limited mobility of the majority of the oligomers is more difficult to rationalize. In further experiments, Calamai *et al*. found that quantum-dot labeled Aβ42 oligomers bound to synthetic giant unilamellar vesicles (GUV's) were much more highly mobile, with a median diffusion coefficient of 1.1×10^{-1} μm^2/s.[32] This value is only one order of magnitude lower than the 2 μm^2/s value we obtained in FRAP experiments with diffusing monomers on planar lipid bilayers. In more recent single particle tracking experiments, we have obtained similar values for the diffusion coefficients of mobile monomers and dimers on planar lipid membranes (Chang, C. C., unpublished data). These results suggest, as the authors note, that interaction with moieties present only in cells may be responsible for the "confined" type motion of most oligomers.[32]

Cell-bound oligomer motion was also assessed by single particle tracking in one of the studies by Narayan *et al*.[31] For these experiments, an incubation concentration of 1 μM Aβ42 or 2 μM Aβ40 was employed on mouse hippocampal neurons. As previously discussed, Narayan *et al*. did detect a highly mobile population of likely monomers on the membrane in Aβ40-treated samples (estimated diffusion coefficient around 10^{-1} μm^2/s).[31] When only Aβ42 species undergoing FRET (presumed oligomers) were analyzed, 20% of particles had diffusion coefficients (D) clustered around 5×10^{-4} μm^2/s, 35% had D around 3×10^{-3} μm^2/s, and 45% had D around 4×10^{-2} μm^2/s. For Aβ40 species undergoing FRET, 42% of particles had D around 4.5×10^{-3} μm^2/s, and 58% had D around 5×10^{-2} μm^2/s. Overall, diffusion coefficients tended to decrease with oligomer size, indicating that larger oligomers diffused less rapidly. Roughly half of the observed species, overall, had diffusion coefficients more typical of "confined" motion or very slow diffusion. Again, the authors suggest that interaction with a cytoskeletal component or other semi-immobile membrane component may be responsible for this observation.[31]

If Aβ on cell membranes is interacting with specific proteins or other molecules within the membrane, what are the other members of these Aβ-containing complexes? Abundant ensemble data has provided evidence for so-called Aβ receptors and has been discussed elsewhere.[70,72–74] However, some insight has also been gained from further single particle tracking experiments. Briefly, one group found that exposure of rat hippocampal neurons to pre-formed Aβ42 oligomers reduced mobility of synaptic and extrasynaptic mGluR5 receptors, and moreover, Aβ oligomers and mGluR5 receptors appeared to codiffuse or associate.[70] Recent explorations by Calamai *et al*. into amyloid oligomer effects on GM1 gangliosides using single particle tracking showed that the pancreatic amyloid-forming peptide amylin aggregates significantly slowed GM1 diffusion, but Aβ42 did not.[69] These studies illustrate the potential of the single particle tracking technique for further localizing Aβ binding on the cell. Our preliminary studies on fixed cells revealed no colocalization of single Aβ oligomers with presynaptic or postsynaptic markers, but a slight preference for association with dendrites over axons was observed.[62] As imaging and labeling techniques continue to improve, single particle tracking methods will likely provide much more insight into the mechanism behind oligomers' limited motion on the membrane.

Current Limitations

The discussion above demonstrates that single molecule techniques have contributed significant new knowledge of Aβ oligomers and their membrane interactions. However, we note that these techniques, like all research methods, do have their limits. Particularly in neuronal primary cells, autofluorescence can present significant challenges to the detection of single fluorophores on the cell surface. This obstacle can generally be overcome by focusing on regions of the cell with low autofluorescence (for example, neurites), using techniques that illuminate only thin sections of the cell (confocal or TIRF geometries), and working with long-wavelength fluorophores when possible (e.g., HiLyte Fluor 647). A more unexpected roadblock has been the lack of observable Aβ-induced toxicity at the physiological concentrations and brief time scales often required for these techniques. Of the studies reviewed here, none have reported correlation between specific oligomeric species and cellular toxicity. This may simply be a result of the previously discussed insensitivity of current methods of assessing toxicity. Alternately, SMM experiments have hitherto utilized mainly synthetic Aβ, and it is possible that endogenous Aβ has chemical or structural characteristics or undergoes modifications which render it significantly more toxic than synthetically prepared peptide. Purifying and labeling endogenous Aβ would likely alter these traits. Using fluorescently labeled antibodies or other external labeling agents on endogenous Aβ is a promising technique. However, no antibodies to specific stoichiometric species exist to our knowledge. In addition to these concerns, the protocols required for observable binding can be harsh and may in some cases require long out-of-incubator time periods, making cell viability and membrane integrity a concern even in control-treated cells.[31]

Certain potential pitfalls are inherent to the use of fluorescently labeled peptides as well. Fluorescent tags could in theory significantly alter the behavior of the Aβ peptide. Data to date suggests that N-terminal tags do not introduce any changes detectable by traditional methods of monitoring aggregation or membrane permeabilization,[8,26] but it is essential to remain mindful of the possibility that labels at other locations or with charges or sizes of unusual magnitude may strongly affect oligomerization and fibril formation. Additionally, for any methods which utilize fluorescence intensity to measure oligomer size, it is important to compare lifetimes of aggregates of various sizes to determine whether the fluorescence is reduced by quenching, particularly for large peptide assemblies.[26–28] When used in solution, the cTCCD method requires corrections for the slower diffusion of larger particles, as large aggregates will appear brighter than they should because of increased time spent in the confocal volume.[29]

Conclusions and Future Directions

Despite the limitations of the technique, single molecule microscopy experiments have provided significant insight into Aβ's behavior in solution at physiological concentrations, its direct interactions with model lipid bilayers and living cell membranes, and some of the conditions that may affect its aggregation in a physiological setting.

SMM measurements confirm that at picomolar to low nanomolar concentrations in solution, monomers and very small oligomers dominate the peptide's size distribution. Membrane interactions of the peptides appear to be highly sensitive to solution peptide concentration and membrane composition and geometry. At low solution concentrations (on the order of 1–2 nanomolar), monomers bind to membranes homogeneously and diffuse rapidly. Slow formation of oligomers from association of rapidly diffusing monomers appears to be the dominant oligomer growth mechanism under these conditions, with the processes of binding and oligomerization being very distinct. At higher concentrations (>100 nanomolar) and on the more complex membranes of living cells, distinguishing the two processes becomes more difficult. Direct insertion of solution-formed oligomers may play an increased role, but formation of oligomers from membrane-bound diffusing monomers is also likely to occur more rapidly. In either case, membrane exposure definitely either (A) catalyzes formation of larger oligomers than are present in solution or (B) promotes rapid binding of the largest oligomers from solution once they form, creating an imbalance between the in-solution and on-membrane oligomer size distributions.

From the SMM data, it is unclear whether these larger membrane-bound oligomers can effectively disrupt normal cellular processes. Species greater than hexamers induce conductivity of model membranes, and neuroblastoma cells do exhibit some low-level, sporadic calcium leakage under conditions in which these oligomers are observed.[26,27] However, the leakage is of much lower magnitude than that observed by previous groups at higher Aβ concentration and using peptide treated with the membrane-toxic solvent hexafluoroisopropanol (HFIP).[17] In preliminary experiments with rat hippocampal neurons, no peptide-induced changes were observed in calcium transient frequency, spine density, or intracellular calcium concentrations. It may be that previous metabolic insults or aging-related inflammatory changes are necessary for neurons to become susceptible to oligomer-mediated toxicity at the peptide concentrations used for SMM experiments.

Single particle tracking experiments by multiple groups have documented that 50–70% of live cell membrane bound oligomers are relatively immobile or "confined" in their diffusion.[31,32,62] We have postulated that the immobility of oligomers bound to model membranes is likely due to full insertion

through the lipid bilayers and binding to the underlying glass surfaces.[61] Similar mechanisms may be at work on cells, with fully membrane-integral Aβ oligomers gaining the ability to interact with cytoskeletal elements underlying the membrane. However, there is also potential for surface-bound oligomers to be interacting with any number of membrane-integral protein or lipid-protein complexes. Further experiments will be required to determine which process, if either, is responsible for the peptide's relative immobility. Regardless of the mechanism, an important point is that the same interactions that restrict these oligomers' mobility may stabilize them conformationally. This phenomenon could lengthen "open" times if oligomer aggregates are behaving like ion-conductive pores or channels. It could also stabilize the exposure of aggregation-promoting portions of the oligomers to solution Aβ, increasing membrane-bound oligomers' abilities to act as seeds for further oligomer growth. We note that similar proportions of the oligomers appear to be immobile at the very low exposure concentrations used in our experiments and at the much higher Aβ concentrations used by Narayan *et al*. and Calamai and Pavone.[31,32,62] The mechanism underlying oligomer immobility does not appear to be affected by solution peptide concentration, indicating that "immobile" binding sites become occupied at very low solution peptide concentrations.

SMM experiments have similarly begun to provide very significant insight into the effects of changes in the solution and membrane milieu on oligomerization. Previously identified peptide-like aggregation promoters and inhibitors have chemical effects on very small, physiological-concentration oligomers, which are largely similar to their effects on aggregates of much greater size at higher concentrations.[47] The chaperones clusterin and aβ-crystallin are capable of stabilizing these oligomers and slightly larger ones.[30,52] These experiments illustrate the power of SMM methods for comparing the effectiveness of different aggregation modifiers on peptide in solution, before any interactions with membranes. Single-molecule FRET studies have conclusively demonstrated that formation of heterogeneous, mixed Aβ40, and Aβ42 oligomers does occur, and these mixed oligomers can act as seeds for downstream binding of more Aβ42, potentiating greater oligomer growth than occuring with either peptide alone.[28] This study illustrates the potential of the method for further exploration into Aβ's interactions with other peptides and membrane components.

The future of single molecule methods in the study of Aβ holds significant promise. With the strong grounding we have discussed here, further development of these techniques could proceed in a number of directions. Our ability to detect membrane-bound Aβ currently supersedes our ability to detect oligomer-induced toxicity. More sensitive methods of detecting Aβ-induced changes to normal physiology need to be developed, so that single membrane-bound oligomers can be correlated with specific localized toxic effects. One group has already utilized an optical patch-clamping method to identify Aβ-induced sites of calcium leakage on frog oocytes.[60] This method could be combined with single-molecule imaging of the cellbound Aβ aggregates to assess the size of specific oligomers inducing leakage. SMM could also be combined with single-channel patch clamping for similar purposes, or with fluorescence-based assessment of dendritic spine structure over time. The Aβ40/Aβ42 relationship should be further explored, and other possible protein or lipid "seeds" or binding partners for Aβ should be studied at physiological concentrations using SMM. Finally, the reasons for oligomers' apparent immobility on membranes should be further explored, as the responsible interactions may be directly or indirectly related to the oligomers' toxicity. Many avenues are open for further study, and single-molecule fluorescence techniques represent a powerful tool for ongoing research into the molecular-level role of Aβ in the development of Alzheimer's disease.

References

1. Crouch PJ, Harding S-ME, White AR, Camakaris J, Bush AI, Masters CL (2008) Mechanisms of Aβ mediated neurodegeneration in Alzheimer's disease. Int J Biochem Cell Biol 40:181–198.
2. McLean CA, Cherny RA, Fraser FW, Fuller SJ, Smith MJ, Beyreuther K, Bush AI, Masters CL (1999) Soluble pool of Aβ amyloid as a determinant of severity of neurodegeneration in Alzheimer's disease. Ann Neurol 155:853–866.
3. Lue L, Kuo Y, Roher A, Brachova L (1999) Soluble amyloid β peptide concentration as a predictor of synaptic change in Alzheimer's disease. Am J Pathol 155: 853–862.
4. Lazo ND, Grant MA, Condron MC, Rigby AC, Teplow DB (2005) On the nucleation of amyloid β-protein monomer folding. Protein Sci 14:1581–1596.
5. Vivekanandan S, Brender JR, Lee SY, Ramamoorthy A (2011) A partially folded structure of amyloid-beta(1–40) in an aqueous environment. Biochem Biophys Res Commun 411:312–316.
6. Bitan G, Kirkitadze MD, Lomakin A, Vollers SS, Benedek GB, Teplow DB (2003) Amyloid β-protein (Aβ) assembly: Aβ40 and Aβ42 oligomerize through distinct pathways. Proc Natl Acad Sci USA 100:330–335.
7. Bitan G, Lomakin A, Teplow DB (2001) Amyloid β-protein oligomerization: prenucleation interactions revealed by photo-induced cross-linking of unmodified proteins. J Biol Chem 276:35176–35184.
8. Ding H, Wong PT, Lee EL, Gafni A, Steel DG (2009) Determination of the oligomer size of amyloidogenic protein β-amyloid(1–40) by single-molecule spectroscopy. Biophys J 97:912–921.
9. Cipriani G, Dolciotti C, Picchi L, Bonuccelli U (2011) Alzheimer and his disease: a brief history. Neurol Sci 32:275–279.

10. Klein WL, Krafft GA, Finch CE (2001) Targeting small Aβ oligomers: the solution to an Alzheimer's disease conundrum? Trends Neurosci 24:219–224.
11. Walsh DM, Selkoe DJ (2007) Aβ oligomers–a decade of discovery. J Neurochem 101:1172–1184.
12. Benilova I, Karran E, De Strooper B (2012) The toxic Aβ oligomer and Alzheimer's disease: an emperor in need of clothes. Nat Neurosci 15:349–357.
13. Davis DG, Schmitt FA, Wekstein DR (1999) Alzheimer neuropathologic alterations in aged cognitively normal subjects. J Neuropathol Exp Neurol 58:376–388.
14. Terry RD, Masliah E, Salmon DP, Butters N, DeTeresa R, Hill R, Hansen L A, Katzman R (1991) Physical basis of cognitive alterations in Alzheimer's disease: synapse loss is the major correlate of cognitive impairment. Ann Neurol 30:572–580.
15. De Meyer G, Shapiro F, Vanderstichele H, Vanmechelen E, Engelborghs S, De Deyn PP, Coart E, Hansson O, Minthon L, Zetterberg H, Blennow K, Shaw L, Trojanowski JQ (2010) Diagnosis-independent Alzheimer disease biomarker signature in cognitively normal elderly people. Arch Neurol 67:949–956.
16. Ono K, Condron MM, Teplow DB (2009) Structure-neurotoxicity relationships of amyloid β-protein oligomers. Proc Natl Acad Sci USA 106:14745–14750.
17. Demuro A, Mina E, Kayed R, Milton SC, Parker I, Glabe CG (2005) Calcium dysregulation and membrane disruption as a ubiquitous neurotoxic mechanism of soluble amyloid oligomers. J Biol Chem 280:17294–17300.
18. Chafekar SM, Baas F, Scheper W (2008) Oligomer-specific Aβ toxicity in cell models is mediated by selective uptake. Biochim Biophys Acta 1782:523–531.
19. Lord SJ, Lee HD, Moerner WE (2010) Single-molecule spectroscopy and imaging of biomolecules in living cells. Anal Chem 82:2192–2203.
20. Walter NG, Huang C, Manzo AJ, Sobhy MA (2008) Do-it-yourself guide: how to use the modern single-molecule toolkit. Nat Methods 5:475–489.
21. Wong PT, Schauerte JA, Wisser KC, Ding H, Lee EL, Steel DG, Gafni A (2009) Amyloid-β membrane binding and permeabilization are distinct processes influenced separately by membrane charge and fluidity. J Mol Biol 386:81–96.
22. Calderon RO, Attema B, DeVries GH (1995) Lipid composition of neuronal cell bodies and neurites from cultured dorsal root ganglia. J Neurochem 64:424–429.
23. Okabe S (2007) Molecular anatomy of the postsynaptic density. Mol Cell Neurosci 34:503–518.
24. Von Bohlen Und Halbach O (2009) Structure and function of dendritic spines within the hippocampus. Ann Anat 191:518–531.
25. Dukes KD, Rodenberg CF, Lammi RK (2008) Monitoring the earliest amyloid-β oligomers via quantized photobleaching of dye-labeled peptides. Anal Biochem 382: 29–34.
26. Schauerte JA, Wong PT, Wisser KC, Ding H, Steel DG, Gafni A (2010) Simultaneous single-molecule fluorescence and conductivity studies reveal distinct classes of Aβ species on lipid bilayers. Biochemistry 49:3031–3039.
27. Johnson RD, Schauerte J A, Wisser KC, Gafni A, Steel DG (2011) Direct observation of single amyloid-β(1–40) oligomers on live cells: binding and growth at physiological concentrations. PLoS One 6:e23970.
28. Chang C-C, Althaus JC, Carruthers CJL, Sutton M A, Steel DG, Gafni A (2013) Synergistic interactions between Alzheimer's Aβ40 and Aβ42 on the surface of primary neurons revealed by single molecule microscopy. PLoS One 8:e82139.
29. Orte A, Birkett NR, Clarke RW, Devlin GL, Dobson CM, Klenerman D (2008) Direct characterization of amyloidogenic oligomers by single-molecule fluorescence. Proc Natl Acad Sci USA 105:14424–14429.
30. Narayan P, Orte A, Clarke RW, Bolognesi B, Hook S, Ganzinger K A, Meehan S, Wilson MR, Dobson CM, Klenerman D (2012) The extracellular chaperone clusterin sequesters oligomeric forms of the amyloid-β(1–40) peptide. Nat Struct Mol Biol 19:79–83.
31. Narayan P, Ganzinger KA, McColl J, Weimann L, Meehan S, Qamar S, Carver JA, Wilson MR, St George-Hyslop P, Dobson CM, et al. (2013) Single molecule characterization of the interactions between amyloid-β peptides and the membranes of hippocampal cells. J Am Chem Soc 135:1491–1498.
32. Calamai M, Pavone FS (2011) Single molecule tracking analysis reveals that the surface mobility of amyloid oligomers is driven by their conformational structure. J Am Chem Soc 133:12001–12008.
33. Li S, Hong S, Shepardson NE, Walsh DM, Shankar GM, Selkoe D (2009) Soluble oligomers of amyloid β protein facilitate hippocampal long-term depression by disrupting neuronal glutamate uptake. Neuron 62:788–801.
34. Shankar GM, Li S, Mehta TH, Garcia-Munoz A, Shepardson NE, Smith I, Brett FM, Farrell MA, Rowan MJ, Lemere CA, et al. (2008) Amyloid-β protein dimers isolated directly from Alzheimer's brains impair synaptic plasticity and memory. Nat Med 14:837–842.
35. Klein WL (2002) Aβ toxicity in Alzheimer's disease: globular oligomers (ADDLs) as new vaccine and drug targets. Neurochem Int 41:345–352.
36. Lacor PN, Buniel MC, Chang L, Fernandez SJ, Gong Y, Viola KL, Lambert MP, Velasco PT, Bigio EH, Finch CE, et al. (2004) Synaptic targeting by Alzheimer's-related amyloid β oligomers. J Neurosci 24:10191–10200.
37. Lacor P, Buniel M, Furlow P (2007) Aβ oligomer-induced aberrations in synapse composition, shape, and density provide a molecular basis for loss of connectivity in Alzheimer's disease. J Neurosci 27:796–807.
38. Zempel H, Thies E, Mandelkow E, Mandelkow E-M (2010) Aβ oligomers cause localized Ca(2+) elevation, missorting of endogenous Tau into dendrites, Tau phosphorylation, and destruction of microtubules and spines. J Neurosci 30:11938–11950.
39. Capone R, Quiroz FG, Prangkio P, Saluja I, Sauer AM, Bautista MR, Turner RS, Yang J, Mayer M (2009) Amyloid-β-induced ion flux in artificial lipid bilayers and neuronal cells: resolving a controversy. Neurotox Res 16:1–13.
40. Lesné S, Koh MT, Kotilinek L, Kayed R, Glabe CG, Yang A, Gallagher M, Ashe KH (2006) A specific amyloid-beta protein assembly in the brain impairs memory. Nature 440:352–357.
41. McDonald JM, Savva GM, Brayne C, Welzel AT, Forster G, Shankar GM, Selkoe DJ, Ince PG, Walsh DM (2010) The presence of sodium dodecyl sulphate-stable Aβ dimers is strongly associated with Alzheimer-type dementia. Brain 133:1328–1341.
42. Arispe N, Rojas E, Pollard HB (1993) Giant multilevel cation channels formed by Alzheimer disease. Proc Natl Acad Sci USA 90:10573–10577.
43. Kawahara M, Arispe N, Kuroda Y, Rojas E (1997) Alzheimer's disease amyloid β-protein forms Zn(2+)-sensitive, cation-selective channels across excised membrane patches from hypothalamic neurons. Biophys J 73:67–75.

44. Lashuel HA, Hartley D, Petre BM, Walz T, Jr PTL, Turner J, King JC, Lachlan-cope TA, Jones PD (2002) Amyloid pores from pathogenic mutations. Nature 418: 291.
45. Lashuel HA, Lansbury PT (2006) Are amyloid diseases caused by protein aggregates that mimic bacterial pore-forming toxins? Q Rev Biophys 39:167–201.
46. Quist A, Doudevski I, Lin H, Azimova R, Ng D, Frangione B, Kagan B, Ghiso J, Lal R (2005) Amyloid ion channels: a common structural link for protein-misfolding disease. Proc Natl Acad Sci USA 102: 10427–10432.
47. Powell LR, Dukes KD, Lammi RK (2012) Probing the efficacy of peptide-based inhibitors against acid- and zinc-promoted oligomerization of amyloid-β peptide via single-oligomer spectroscopy. Biophys Chem 160:12–19.
48. Pallitto MM, Ghanta J, Heinzelman P, Kiessling LL, Murphy RM (1999) Recognition sequence design for peptidyl modulators of β-amyloid aggregation and toxicity. Biochemistry 38:3570–3578.
49. Soto C, Sigurdsson E, Morelli L, Kumar R, Castano E, Frangione B (1998) β-sheet breaker peptides inhibit fibrillogenesis in a rat brain model of amyloidosis: implications for Alzheimer's disease. Nat Med 4:822–826.
50. Gordon DJ, Sciarretta KL, Meredith SC (2001) Inhibition of beta-amyloid(40) fibrillogenesis and disassembly of beta-amyloid (40) fibrils by short beta-amyloid congeners containing N-methyl amino acids at alternate residues. Biochemistry 40:8237–8245.
51. Etienne M A, Aucoin JP, Fu Y, McCarley RL, Hammer RP (2006) Stoichiometric inhibition of amyloid beta-protein aggregation with peptides containing alternating alpha,alpha-disubstituted amino acids. J Am Chem Soc 128:3522–3523.
52. Narayan P, Meehan S, Carver J A, Wilson MR, Dobson CM, Klenerman D (2012) Amyloid-β oligomers are sequestered by both intracellular and extracellular chaperones. Biochemistry 51:9270–9276.
53. Dahlgren KN, Manelli AM, Stine WB, Baker LK, Krafft GA, LaDu MJ (2002) Oligomeric and fibrillar species of amyloid-β peptides differentially affect neuronal viability. J Biol Chem 277:32046–32053.
54. Simakova O, Arispe NJ (2006) Early and late cytotoxic effects of external application of the Alzheimer's Aβ result from the initial formation and function of Aβ ion channels. Biochemistry 45:5907–5915.
55. Jan A, Gokce O, Luthi-Carter R, Lashuel HA (2008) The ratio of monomeric to aggregated forms of Aβ40 and Aβ42 is an important determinant of amyloid-β aggregation, fibrillogenesis, and toxicity. J Biol Chem 283:28176–28189.
56. Kuperstein I, Broersen K, Benilova I, Rozenski J, Jonckheere W, Debulpaep M, Segers-nolten I, Werf K Van Der, Subramaniam V, Braeken D, et al. (2010) Neurotoxicity of Alzheimer's disease Aβ peptides is induced by small changes in the Aβ42 to Aβ40 ratio. EMBO J 29:3408–3420.
57. Li S, Jin M, Koeglsperger T, Shepardson NE, Shankar GM, Selkoe DJ (2011) Soluble Aβ oligomers inhibit long-term potentiation through a mechanism involving excessive activation of extrasynaptic NR2B-containing NMDA receptors. J Neurosci 31:6627–6638.
58. Varghese K, Molnar P, Das M, Bhargava N, Lambert S, S M, Hickman JJ (2010) A new target for amyloid beta toxicity validated by standard and high-throughput electrophysiology. Changes 5:1–8.
59. Wu H-Y, Hudry E, Hashimoto T, Kuchibhotla K, Rozkalne A, Fan Z, Spires-Jones T, Xie H, Arbel-Ornath M, Grosskreutz CL, et al. (2010) Amyloid β induces the morphological neurodegenerative triad of spine loss, dendritic simplification, and neuritic dystrophies through calcineurin activation. J Neurosci 30:2636–2649.
60. Demuro A, Smith M, Parker I (2011) Single-channel Ca(2+) imaging implicates Aβ1–42 amyloid pores in Alzheimer's disease pathology. J Cell Biol 195:515–524.
61. Ding H, Schauerte J A, Steel DG, Gafni A (2012) β-Amyloid (1–40) peptide interactions with supported phospholipid membranes: a single-molecule study. Biophys J 103:1500–1509.
62. Johnson RD, Schauerte J A, Chang C-C, Wisser KC, Althaus JC, Carruthers CJL, Sutton M A, Steel DG, Gafni A (2013) Single-molecule imaging reveals aβ42: aβ40 ratio-dependent oligomer growth on neuronal processes. Biophys J 104:894–903.
63. Zhang Y-J, Shi J-M, Bai C-J, Wang H, Li H-Y, Wu Y, Ji S-R (2012) Intra-membrane oligomerization and extra-membrane oligomerization of amyloid-β peptide are competing processes as a result of distinct patterns of motif interplay. J Biol Chem 287:748–756.
64. Kumar-singh S, Theuns ÃJ, Broeck B Van , Pirici D, Vennekens K, Corsmit E, Cruts M, Dermaut B, Wang R, Broeckhoven C Van (2006) Mean age-of-onset of familial Alzheimer disease caused by presenilin mutations correlates with both increased Aβ42 and decreased Aβ40. Hum Mutat 27:686–695.
65. Walker ES, Martinez M, Brunkan AL, Goate A (2005) Presenilin 2 familial Alzheimer's disease mutations result in partial loss of function and dramatic changes in Aβ 42/40 ratios. J Neurochem 92:294–301.
66. Duff K, Eckman C, Zehr C, Yu X, Prada C (1996) Increased amyloid-β42(43) in brains of mice expressing mutant presenilin 1. Nature 383:710–713.
67. Citron M, Westaway D, Xia W, Carlson G (1997) Mutant presenilins of Alzheimer's disease increase production of 42-residue amyloid β-protein in both transfected cells and transgenic mice. Nat Med 3:67–72.
68. Borchelt DR, Thinakaran G, Eckman CB, Lee MK, Davenport F, Ratovitsky T, Prada C, Kim G, Seekins S, Yager D, et al. (1996) Familial Alzheimer's disease – linked presenilin 1 variants elevate Aβ1–42/1–40 ratio in vitro and in vivo. Neuron 17:1005–1013.
69. Calamai M, Pavone FS (2013) Partitioning and confinement of GM1 ganglioside induced by amyloid aggregates. FEBS Lett 587:1385–1391.
70. Renner M, Lacor PN, Velasco PT, Xu J, Contractor A, Klein WL, Triller A (2010) Deleterious effects of amyloid β oligomers acting as an extracellular scaffold for mGluR5. Neuron 66:739–754.
71. Omtri R, Davidson M (2012) Differences in the cellular uptake and intracellular itineraries of amyloid beta proteins 40 and 42: Ramifications for the Alzheimer's drug discovery. Mol Pharm 9:1887–1897.
72. Wang H, Lee DHS, Andrea MRD, Peterson PA, Shank RP, Reitz AB (2000) β-amyloid 1–42 binds to α7 nicotinic acetylcholine receptor with high affinity. J Biol Chem 275:5626–5632.
73. Laurén J, Gimbel DA, Nygaard HB, Gilbert JW, Strittmatter SM (2009) Cellular prion protein mediates impairment of synaptic plasticity by amyloid-β oligomers. Nature 457:1128–1132.
74. Cisse M, Halabisky B, Harris J, Devidze N, Dubal DB, Sun B, Orr A, Lotz G, Kim DH, Hamto P, et al. (2011) Reversing EphB2 depletion rescues cognitive functions in Alzheimer model. Nature 469:47–52.